The carnivoran adaptive landscape reveals trade-offs among functional traits in the skull, appendicular, and axial skeleton

Chris J. Law[1,2,3], Leslea J. Hlusko[4], Z. Jack Tseng[3]

[1]Department of Integrative Biology, University of Texas

[2]Burke Museum and Department of Biology, University of Washington

[3]Department of Integrative Biology, University of California Berkeley

[4]National Research Center on Human Evolution (CENIEH), Burgos, Spain

Abstract

Analyses of form-function relationships are widely used to understand links between morphology, ecology, and species fitness across macroevolutionary scales. However, few have investigated functional trade-offs and covariance among functional traits within and between the skull, limbs, and vertebral column simultaneously. In this study, we investigated the adaptive landscape of skeletal form and function in carnivorans to test how functional trade-offs between these skeletal regions contribute to ecological adaptations and the topology of the landscape. We found that functional traits derived from carnivoran skeletal regions exhibit trade-offs and covariation across their performance surfaces, particularly in the appendicular and axial skeletons. These functional trade-offs and covariation corresponded as specializations to different adaptive landscapes when optimized by locomotor mode, diet, or family. Lastly, we found that the topologies of the optimized adaptive landscapes and underlying performance surfaces are largely characterized as smooth, gradual gradients between regions of low and high

adaptive zones rather than as rugged, multipeak landscapes. Our results suggest that carnivorans may already occupy a broad adaptive zone as part of a larger mammalian adaptive landscape that masks the form and function relationships of skeletal traits.

Key words: Adaptive peak, Carnivora, ecomorphology, functional morphology, phylogenetic comparative methods

Introduction

The diversity of animal forms is one of the most salient patterns across the tree of life, and how morphological variation relates to the ecological diversity and survival of species across macroevolutionary time remains a core question in evolutionary biology. The varying strength of form–function relationships has provided biologists with insight into the specificity of morphological structure in determining species' abilities to carry out ecological tasks (i.e., performances), especially when behavioral observations are scarce. Thus, performance is considered the link between morphology, ecology, and species fitness [1–3]. Although many studies have examined the form-function relationship of the skull [4–7], appendicular skeleton [8–11], and axial skeleton [12–16], few have investigated functional trade-offs and covariation among these three major skeletal systems.

The rise of adaptive landscape analyses has enabled researchers to investigate the adaptive evolution of performance by elucidating the underlying links among morphology, ecology, and fitness benefits (i.e., adaptiveness) at the macroevolutionary level [17]. Ornstein–Uhlenbeck (OU) models [18–22] are widely used to test for the presence of adaptive zones or peaks (e.g., [7,23–28]. However, it remains difficult to characterize the full topology (i.e., peaks, valleys, and slope) of the adaptive landscape as well as assess the relative importance of multiple

performance traits and their contributions to overall adaptive fitness using these models. Functional adaptive landscape analyses [11,15,29] can overcome these limitations by examining the distribution of species in morphospace and its relationship to the relative importance of various functional traits on the topology of the adaptive landscape. Nevertheless, while an increasing number of studies have used functional adaptive landscapes to examine links between morphological diversity and functional performance [6,11,13,15,16,29], no study has yet to investigate functional trade-offs and covariation among the skull, limbs, and vertebral column.

Here, we investigate the adaptive landscape of skeletal form and function in carnivorans to test how functional trade-offs contribute to ecological adaptations and the topology of the landscape. We use carnivorans (e.g., bears, cats, dogs, seals, and their relatives) as our model system to examine the evolution of skeletal form and function because of their high species richness and broad morphological and ecological diversity. In terms of skeletal diversity, numerous studies have investigated the morphology of the carnivoran skull [4,30–35], appendicular skeleton [36–41], vertebral column [42–44], and overall body plan [23,45,46]. This morphological diversity is attributed to mosaic evolution, in which different skeletal components exhibit distinct modes of evolution either from phylogenetic natural history or from selection through ecological adaptations [47]. The ability of individual skeletal components to adapt to specific ecological factors independently from each other may have contributed to the clade's hierarchical evolution. The hierarchical evolution is primarily framed by dental adaptations along an axis of dietary resource use, which are hypothesized to facilitate the early radiation of carnivorans across a rugged, multi-peak adaptive landscape [33]. Subsequent evolution led to the continual partitioning between clades, resulting in the origination of extant carnivoran families that occupy different adaptive zones [48] with distinct morphologies in the skull, appendicular,

and axial skeletons [34,45,47]. Skeletal variation in the mandible, hindlimb, and post-diaphragmatic region of the vertebral column then arose along shared ecological axes among taxa, theoretically leading to distinct ecological peaks across the adaptive landscape [34,47].

However, the functional implications of these skeletal traits remain to be tested, albeit OU modeling provided evidence that appendicular functional traits exhibit relatively low ruggedness across the adaptive landscape despite also exhibiting distinct adaptive peaks [23]. Thus, the interpretation of the ruggedness of the adaptive landscape or steepness of adaptive peaks remains difficult to ascertain using OU models and may depend on different ecological contexts as well as the use of either morphological or functional traits. In this study, we advance the investigation of the carnivoran adaptive landscape using functional landscape analyses to investigate the functionality of the skull, appendicular, and axial skeletons simultaneously. We have three goals: 1) assess if performance surfaces reveal trade-offs among functional traits from the skull, appendicular, and axial skeleton; 2) test for unique adaptive landscapes along locomotor, dietary, and phylogenetic axes and assess how functional traits from various skeletal components contribute to these landscapes; and 3) examine the topologies of the adaptive landscapes to provide further insight on carnivoran evolution.

Methods

Morphospace and functional traits

We created a morphospace of 109 terrestrial carnivoran species from 198 specimens based on 136 linear and angular measurements that capture morphological variation across the entire skeleton (Fig. S1). This dataset includes seven cranial traits, seven mandibular traits, 13 forelimb traits, 13 hindlimb traits, and 11 traits each in the third cervical, fifth cervical, first thoracic, middle thoracic, diaphragmatic thoracic, last thoracic, first lumbar, middle lumbar and

last lumbar vertebrae. We were able to incorporate representatives from 12 of the 13 extant terrestrial carnivoran families; specimens from Prionodontidae were unavailable. We removed size effects on linear measurements by calculating the log shape ratio (i.e., ln[trait/size]) of each skeletal trait, where size is the geometric mean of all linear trait measurements. We used only adult male specimens because carnivorans exhibit differing degrees of sexual dimorphism (Law 2019). We then conducted a principal component analysis (PCA) on all size-corrected measurements and used the first two PC axes (46.7% of the total variance) to create the morphospace (Fig. 1; see Table S1 for PC loadings). Carnivoran species are widely distributed across the morphospace except for the bottom-left region in which no species occupy (-PC1, -PC2).

To fully sample skeletal variation throughout the morphospace, we generated theoretical morphological traits evenly across the morphospace in a 7 x 5 grid by multiplying each eigenvector by each specified PC score and adding the mean of all 136 traits. From these theoretical morphological traits, we calculated 42 functional traits that capture the functional diversity of the skull [49], limbs [39,50], and vertebral column [13,51,52] (Table 1). The variance of each functional trait was scaled from 0 to 1 to standardize the functional data.

Ecological traits

We classified the 109 carnivoran species into one of seven locomotor regimes: arboreal (species that primarily live in trees and rarely come down to the ground), cursorial (species that displays rapid bounding locomotion), scansorial (species that spend equal time in trees and on the ground), semi-aquatic (species that regularly swim for dispersal and/or foraging), semi-fossorial (species that regularly dig for shelter and/or foraging), and terrestrial (species that primarily live on the ground and rarely climb, dig, or swim). Terrestrial species were further

categorized as terrestrial hunters (species that exhibit ambush and/or pouncing behaviors to kill prey) and terrestrial non-hunters (species that rarely hunt for prey). We also classified each species into one of seven dietary regimes: large prey hypercarnivory (consist of >70% terrestrial vertebrate prey that exceeds the predator's own body mass), medium prey hypercarnivory (consist of >70% terrestrial vertebrate prey that are up to the predator's own body mass), small prey hypercarnivory (consist of >70% terrestrial vertebrate prey that are up to 20% of the predator's own body mass), omnivory (consist of >50% terrestrial vertebrates), insectivory (consisting of >70% invertebrates), aquatic carnivory (consist of >90% aquatic prey), and herbivory (consist of >90% plant material). Definitions for locomotor and dietary regimes were obtained from [34,45] with minor edits based on literature review.

Adaptive Landscapes

We investigated the functional optimality of the skeleton using adaptive landscape analyses [11,13,15,29]. All adaptive landscapes were computed using the R package Morphoscape [29]. We first created performance surfaces by interpolating each functional trait across the morphospace surface using ordinary kriging. We then computed a combined adaptive landscape (W) as the summation of individual performance surfaces (F_n), each weighted by their relative importance or contribution to overall fitness (w_n) [15]:

$$W = w_1F_1 + w_2F_2 + \bullet\bullet\bullet + w_nF_n$$

where W is optimized as the likelihood of combinations of performance surface and relative fitness, under the definition that the total fitness sums to 1 and the variance of all surfaces is equal. Due to computational demands, we had to reduce the number of functional traits from 42 to 27 to compute the combined adaptive landscape. Because the carnivoran vertebral column can be divided into three regionalized modules (i.e., cervical, pre-diaphragmatic thoracic, and post-

diaphragmatic thoracolumbar) with the diaphragmatic vertebra serving as a transitional vertebra [44], we only included the functional traits of the fifth cervical vertebrae, middle thoracic vertebrae, diaphragmatic vertebrae, and middle lumbar vertebrae as our proxies for these four regions and excluded the remaining vertebral functional traits in subsequent analyses. For these 27 functional traits, we tested all possible combinations of weights, ranging from 0 to 1 in increments of 0.25, across a total of 27,405 possible adaptive landscapes. We were unable to partition weights with smaller increments due to the number of functional traits used.

Lastly, we identified the optimally weighted landscape that maximizes the fitness of each locomotor regime using the function calcWprimeBy, and tested whether these optimal landscapes are significantly different among locomotor ecological groups using the function multi.lands.grp.test. Significance testing was performed by comparing the number of landscapes shared by the top percentile of each group with the total number of landscapes in this top percentile. The top percentile of each group was determined using a chi-squared test. We also investigated differences in adaptive landscapes among dietary groups and carnivoran families that contained more than one species.

Results

Performance surfaces reveal functional trade-offs

Each functional trait mapped onto the morphospace revealed both unique and similar performance surfaces that characterize trait groups, suggesting that functional trade-offs and covariation are present within and among skeletal systems. In the skull, mechanical advantage of jaw closure tends to be greatest in the bottom of morphospace, with temporalis mechanical advantage (temMA) highest towards the bottom-left (-PC1, -PC2) and declining towards the top-

right (+PC1, +PC2) whereas masseter mechanical advantage (masMA) is highest towards the bottom-right (+PC1, -PC2) and declines towards the top-left (-PC1, +PC2) (Fig. 2).

In the forelimb, there is a trade-off between limb elongation and elbow robustness: indices of scapula (SI), radius (BI), and metacarpal (MAN) elongation are highest in the top-right (+PC1, +PC2) of morphospace and transitions towards increased robustness diagonally to the bottom-left (-PC1, -PC2). Indices associated with increased mechanical advantage of elbow extension (OLI) and attachment sites for forearm flexor, pronator, and supinator muscles on the humeral epicondyles (HEI) and ulna (URI) exhibit the opposite pattern (i.e., highest in the bottom-left and lowest in the top-right). Overall robustness of humerus (HRI) is highest on the left side of the morphospace (-PC1) and transitions towards increased elongation to the right (+PC1), following a similar distribution as the latter indices. The hindlimb also exhibits a trade-off between elongation and robustness: indices of tibial (CI) and metatarsal (PES) elongation tend to be highest in the right side (+PC1, with CI also trending towards -PC2) and transitions to increased robustness towards to the left side (-PC2), whereas indices for femoral (FEI, FRI) and tibial (TRI) robustness tend to be highest on the left side (-PC1) but transitions towards less robustness on PC2 (FEI and FRI is highest towards -PC2 and TRI is highest towards +PC2).

Lastly, in the vertebral joints, there is a trade-off between range of rotational motion and sagittal mobility: for the cervical, diaphragmatic, and lumbar joints, joint torsional angle (JTA) as a proxy for range of rotational motion is highest in the bottom-left of the morphospace (-PC1, -PC2) and declines diagonally to the top-right (+PC1, +PC2), whereas joint verticality (JV) as a proxy for sagittal mobility exhibit the opposite pattern (i.e., highest in the top-right and lowest in the bottom-left). The thoracic vertebra exhibits similar JTA and JV distributions but in the horizontal plane (i.e., highest JTA in the left side of morphospace and highest JV in the right).

Stiffness of all vertebral joints (SMA) tends to be greatest towards the top-left of morphospace (-PC1, +PC2) and declines towards the right side of morphospace (+PC1).

Optimized Adaptive Landscapes

After summation of all performance surfaces based on optimized weights, we found that the combined adaptive landscape is heavily weighted for sagittal mobility of the pre-diaphragmatic thoracic region (w_{JV} = 0.71; Fig. 3A; Table S2). When adaptive landscapes are optimized by locomotor ecologies, we found different degrees to which the 27 functional traits are incorporated among the different adaptive landscapes. The cursorial landscape is characterized by evenly weighted functional traits associated with increased sagittal mobility of the vertebral column (w_{JV} = 0.14–0.15 for the cervical, pre-diaphragmatic thoracic, diaphragmatic, and lumbar regions) and lengthening of the forelimb, particularly in the scapula (w_{SI} = 0.10), radius (w_{BI} = 0.15), and metacarpal (w_{MAN} = 0.10) (Fig. 3C; Table S2). This landscape is significantly different from all other locomotor landscapes except with the terrestrial non-hunter landscape (Table 2). Semi-aquatic and semi-fossorial landscapes do not significantly differ from one another (P = 0.917; Table 2), and both are weighted for increased joint torsion in the cervical (w_{JTA} = 0.25), diaphragmatic (w_{JTA} = 0.09), and lumbar (w_{JTA} = 0.22) regions; larger femoral epicondyles (w_{FEI} = 0.25); and enlarged olecranon processes (w_{OLI} = 0.09) (Fig. 3E, F; Table S2). The remaining locomotor landscapes do not significantly differ from one another (Table 2) and are heavily weighted for sagittal mobility of the pre-diaphragmatic thoracic region (w_{JV} = 0.56–0.78; Fig. 3; Table S2).

When adaptive landscapes are optimized by dietary ecologies, we found that differences in landscapes appear associated with carnivory (Fig. S2; Table S3). Adaptive landscapes based on diets that largely consists of terrestrial vertebrate prey (i.e., carnivory and omnivory) are

heavily weighted for sagittal mobility of the pre-diaphragmatic thoracic region (w_{JV} = 0.66–0.73; Fig. S2; Table S4). In contrast, adaptive landscapes based on diets that do not incorporate terrestrial vertebrate prey (i.e., herbivory, insectivory, and piscivory) are characterized by evenly weighted functional traits associated with increased joint torsion in the cervical and lumbar regions and larger femoral epicondyles (Fig. S2; Table S4).

Lastly, we found different adaptive landscapes when they are optimized by family. Adaptive landscapes for felids, viverrids, euplerids, herpestids, and procyonids are not significantly different from each other and all remain heavily weighted for sagittal mobility of the pre-diaphragmatic thoracic region (w_{JV} = 0.55–0.77; Fig. 4; Table 3; Table S5). The canid landscape resembles the cursorial landscape with similar weights for increased sagittal mobility of the pre-diaphragmatic thoracic (w_{JV} = 0.36) and diaphragmatic (w_{JV} = 0.17) joints and lengthening of the scapula (w_{SI} = 0.14) (Fig. 4G; Table S5); however, it does not significantly differ from the above family-specific landscapes (Table 3). The mephitid and mustelid landscapes resemble semi-aquatic and semi-fossorial landscapes with similar weights for larger femoral epicondyles (w_{FEI} = 0.20–0.26) and increased joint torsion in the cervical (w_{JTA} = 0.22–0.26) and lumbar (w_{JTA} = 0.18–0.21) joints (Fig. 4I, K), but only the mephitid landscape significant differs from all other families (Table 3). The hyaenid landscape weighted heavily for increased stiffness of all the cervical joints (w_{SMA} = 0.39) and elongation of the radius (w_{BI} = 0.33) (Fig. 4D), whereas the ursid landscape weighted heavily among increased stiffness of all the vertebral joints ($\sum w_{SMA}$ = 0.54) and increased robustness of the humerus (w_{HRI} = 0.16) and tibia (w_{TRI} = 0.19) (Fig. 4H). Both hyaenid and ursid landscapes significantly differ with all other family-specific landscapes (Table 3).

Discussion

The diversity found in the carnivoran skeletal system is attributed to mosaic evolution, in which the mandible, hindlimb, and post-diaphragmatic vertebrae showed evidence of adaptation towards ecological regimes whereas the cranium, forelimb, and pre-diaphragmatic vertebrae reflect clade-specific evolutionary shift [47]. Using adaptive landscape analyses, we further found that functional traits derived from this morphological diversity exhibit trade-offs and covariation across their performance surfaces, particularly in the appendicular and axial skeletons. These functional trade-offs and covariation correspond as adaptations to different adaptive landscapes when optimized by various factors including phylogeny, dietary ecology, and, in particular, locomotor mode. Lastly, these adaptive landscapes and underlying performance surfaces are characterized by rather broad slopes, hinting that carnivorans occupy a broad adaptive zone as part of a larger mammalian adaptive landscape that masks the form and function relationships of skeletal traits.

Performance surfaces reveal trade-offs among functional traits

In the appendicular skeleton, we confirm hypotheses that the gradient from gracility to robustness often found as the primary source of variation across limb bone morphospace [40,41,53–57] signifies a functional trade-off between increasing cost of transport associated with cursoriality and resisting stresses associated with locomoting through resistant media (Fig. 2B). Specifically, long, gracile limb bones particularly on the distal ends of the limbs facilitate increased stride length and decreased moment of inertia of limbs, which in turn decreases the energetic cost of transport and increases running speeds [58–64]. In contrast, short, robust limb bones facilitate resistance to bending and shearing stresses and increased mechanical advantage for forceful movements by reducing the out-lever of the limb and increasing the in-lever of muscle forces [65,66]. Robustness also permits increased surface area of the bone for more

muscles to attach. Enlargement of the humeral and femoral epicondyles increases the attachment sites of several musculature (i.e., flexors, pronators, and supinators in the forelimb and gastrocnemius and soleus muscles in hindlimb) responsible for generating power, force, and stability [50,65,67,68]. Additionally, an enlarged olecranon process facilitates stronger extension and flexion of the elbow and wrist by increasing mechanical advantage of the triceps brachii and dorsoepitrochlearis muscles and providing greater attachment sites for the ulnar head of the flexor carpi ulnaris [50,65,67,68]. These adaptations facilitate the ability to generate large forces during certain locomotor behaviors such as digging [39,57,65,67–69] or swimming [39,56,70,71].

In the axial skeleton, we found that carnivorans exhibit trade-offs between joint mobility, range of axial rotation, and, to a lesser extent, stiffness of the vertebral column. That is, high sagittal mobility covaries with low range of axial rotation and low stiffness whereas low sagittal mobility covaries with high range of axial rotation and high stiffness. This pattern is surprising because, compared to other tetrapods, mammals exhibit intervertebral joints that are characterized by high sagittal mobility, high axial rotation, and high stiffness [13]. A possible explanation is that the covariation between high sagittal mobility and low axial rotation may serve as a further adaptation to increasing forward locomotion by prioritizing flexibility in the sagittal plane through the reduction of torsional twisting. High mobility of the backbone in the sagittal plane has long been recognized as a key adaptation facilitating the diversity of different locomotor habits in mammals, particularly asymmetrical gaits (e.g., gallop, half-bound, bound) by enabling extensive dorsoventral flexion of the body axis [72–75]. The reduction of torsional twisting in carnivorans may, therefore, prioritize force generation in the sagittal plane (rather than parasagittal or transverse plane) needed for these locomotor behaviors. Evidence for this

hypothesis is found in comparisons with ungulates, where carnivorans exhibit up to ~38° more sagittal mobility in the lumbar region and up to 200% less axial rotational mobility in the thoracic region compared to ungulates [76–78]. Increased rotational mobility of the backbone in ungulates is hypothesized to enhance agile maneuvering such as sharp cornering and quick directional changes when escaping from predators [78].

We also found that high sagittal mobility loosely covaries with low stiffness of the intervertebral joints, a surprising result considering that stiffness is often hypothesized to help store elastic energy in the back between strides [13,51,79,80]. A possible explanation is that the aponeurosis of the longissimus dorsi muscle and paravertebral muscles serve as more important storage for elastic energy than the backbone [79,81,82]. Alternatively, as mammals [13], carnivorans already exhibit optimally stiff backbones that are sufficient for elastic energy storage for their range of locomotor behaviors. Therefore, selection has not led to increased stiffness, and the majority of carnivorans are distributed close to the valley of the performance surface. Earlier work indicates that carnivorans exhibit lower intervertebral joint stiffness compared to a crab-eating macaque and red-necked wallaby [83], two species with specialized forms of locomotion not found in carnivorans. Thus, additional work is needed to understand how the stiffness of intervertebral joints in carnivorans compare with other mammals.

Functional covariation between appendicular and axial skeletons optimizes the adaptive landscapes of some locomotor ecologies

The optimized adaptive landscape is heavily weighted for sagittal mobility of the pre-diaphragmatic thoracic joints (Fig. 3A), indicating that flexibility in the sagittal plane serves an important functional role for all carnivorans. When the adaptive landscapes are optimized based on locomotor ecology, we found that only cursorial, semi-aquatic, and semi-fossorial landscapes

were significantly different (Fig. 3; Table 2). Correspondingly, the functional trade-offs identified by the performance surfaces are associated with these three locomotor modes, with cursoriality on one end and semi-aquatic and semi-fossorial behaviors, both of which require large force generation from swimming and digging, on the other end. Furthermore, the locomotor-specific landscapes revealed that covariation of the appendicular and axial skeletons facilitate adaptations to each of these locomotor behaviors. These trade-offs are largely independent of size effects because body size variation scales from the top-left to bottom-right of morphospace whereas the trade-offs scale from the top-right to the bottom-left (Fig. 3; Fig. 4; Fig. S2).

The majority of cursorial carnivorans occupy the highest regions of the cursorial landscape. This landscape indicates that the appendicular and axial skeletons of cursorial carnivorans are functionally adapted for increased stride length through elongation of forelimb and increased sagittal flexibility of the full vertebral column (Fig. 3C; Table S2). As described above, these adaptations increase running speeds and reduce the energetic cost of transport by prioritizing dorsoventral flexion and extension in the sagittal plane [58–63,72–75,78].

At the other extreme, the appendicular and axial skeletons of semi-aquatic and semi-fossorial carnivorans are functionally adapted for increased elbow and knee extension through enlarged elements of the limbs and increased axial rotation in the vertebral column (Fig. 3E, F; Table S2). It is well documented that adaptations in the elbows and knees facilitate the ability to generate large power strokes for turning and stabilizing the body while swimming [39,56,70,71]. These similar adaptations also enable semi-fossorial species to generate large forces to dig [39,57,65,67–69] and improve stability and load transfer during clearing [57,65,71,84]. What remains largely undetermined is the importance of increased axial joint rotation during

swimming or digging. Presumably, for swimmers, torsional rotation of the intervertebral joints increases the maneuverability and ability to perform rapid turns in water [85,86]. Fully aquatic seals exhibit more flexible and compliant intervertebral joints compared to terrestrial mammals [83]; whether their joints are also more capable for torsional rotation remains to be studied. For semi-fossorial carnivorans, increased axial rotation of the vertebral column may provide additional leverage when digging through sediment. Evidence for increased axial rotation has been observed in the semi-fossorial nine-banded armadillo; experimentation on intervertebral joint flexion in this species revealed rotational motion in the joints despite not being explicitly tested [87]. Nonetheless, the benefits of increased joint rotation for digging remains puzzling. Interestingly, no carnivorans, including semi-aquatic and semi-fossorial species, occupy the highest regions of semi-aquatic or semi-fossorial landscapes. A likely explanation is that further axial rotation is biologically impossible for these carnivorans given their vertebral morphology that may be under evolutionary constraints having originated from terrestrial carnivorans. Thus, semi-aquatic and semi-fossorial carnivorans may already be at the highest region of the adaptive landscape that is biologically feasible.

The remaining locomotor landscapes are heavily weighted for sagittal mobility of the pre-diaphragmatic thoracic region (Fig. 3; Table S2). That the arboreal landscape was not heavily weighted by additional functional traits is surprising considering that arboreality is often described as a specialized form of locomotion [88]. A possible explanation is that carnivorans do not display the full diversity of arboreal behaviors (e.g., brachiation, leaping, suspensory climbing) performed by other mammals. Another possibility is that we did not include all possible functional traits in our analyses. For example, the ratio between proximal manual phalanx length and metacarpal length has been shown to accurately predict climbing frequency

in rodents [89], and thus may have altered the optimized weights of the arboreal adaptive landscape if this trait or others were included in this current study. These unaccounted sources may also explain why arboreal species lie away from the highest regions of the adaptive landscape (Fig. 3B).

Adaptive landscapes optimized based on family also demonstrate similar patterns as locomotor-specific landscapes (Fig. 4). The majority of family-specific landscapes are heavily weighted for sagittal mobility of the pre-diaphragmatic thoracic region. Canids, which primarily exhibit cursorial or terrestrial hunting behaviors, exhibit similar patterns with the cursorial landscape with increased sagittal mobility in other regions of the vertebral column and elongation of the forelimb (Fig. 4G). Likewise, mephitids and mustelids comprise of many semi-aquatic and semi-fossorial species and thus exhibit similar patterns with the semi-aquatic and semi-fossorial landscapes of increased intervertebral joint rotation and enlarged limb joints (Fig. 4I, K). Adaptive landscapes for hyaenids and ursids are both unique compared to other family-specific landscapes (Table 3). The hyaenid landscape is heavily weighted for relative elongation of the forelimb (Fig. 4D); however, a caveat is that our low sample size of just two species may reflect a biased representation of taxa with elongate forelimb and sloped back found in their extant diversity. Lastly, the ursid landscape is heavily weighted for increased intervertebral joint stiffness of the thoracolumbar vertebrae and increased robustness of the stylopodia of the limbs (Fig. 4H). These results are unsurprising as ursids are the biggest terrestrial carnivorans and these traits support their heavy bodies against the effects of gravity [13,64].

Lastly, we found that adaptive landscapes optimized based on dietary ecology are distinguished from each other based on the presence of terrestrial vertebrate prey in their diets, which in turn can be partially explained by locomotor mode. In carnivorous and omnivorous

carnivorans, a variety of hunting behaviors such as pursuing, ambush, pouncing, and digging behaviors are used to capture prey. Therefore, optimizing the landscape based on just carnivory masks these locomotor specializations and thus our ability to detect trade-offs and covariation among functional traits. As a result, the carnivore and omnivore landscapes cannot be distinguished from the combined landscape and are all heavily weighted for sagittal mobility of the pre-diaphragmatic thoracic region (Fig. S2; Table S4). In contrast, the herbivore, insectivore, and piscivore landscapes are all heavily weighted for increased joint torsion in the cervical and lumbar regions and larger femoral epicondyles (Fig. S2; Table S4), functional traits that are also heavily weighted for semi-aquatic and semi-fossorial carnivorans. These results suggest that adaptations for swimming and digging behaviors not only dictate the functional landscape but may also help facilitate insectivorous and piscivorous diets; that is, they need to swim or dig for their prey. Nevertheless, our functional trait dataset consists of just the mechanical advantage of jaw closure and thus may not capture the full functional diversity found in carnivorans. Inclusion of additional functional traits from the cranium, mandible, and dentition may uncover further important contributions of the skull in the evolution of carnivorans (Tseng and Flynn 2018; Slater 2019; Law et al. 2022; Sansalone et al. 2024).

The carnivorans adaptive landscape is relatively flat

Many carnivoran skeletal components (e.g., mandible, dentition, hindlimb, and post-diaphragmatic region of the vertebral column) exhibit a short phylogenetic half-life relative to the age of Carnivora, suggesting that skeletal traits are strongly pulled towards distinct ecological peaks or clade-based adaptive zones across the adaptive landscape [23,33,34,47]. Surprisingly, we found that the topology of the carnivoran performance surfaces and optimized adaptive landscapes are largely characterized as smooth, gradual gradients between regions of low and

high adaptive zones rather than as rugged, multipeak landscapes. Many-to-one mapping [90] may explain this decoupling between form and function. Multiple combinations of morphological traits may lead to the same functional outcome, resulting in a flat landscape that does not capture the rugged morphological landscape that was previously hypothesized.

The presence of a relatively flat topology may also indicate that carnivorans already occupy a broad adaptive zone relative to the overall mammalian adaptive landscape. Although carnivorans exhibit diverse locomotor modes and correspondingly diverse morphological adaptations, this diversity does not match the extreme locomotor and morphological specialization found in other mammalian clades, especially in the appendicular skeleton such as cranially facing forelimbs in subterranean moles [91], digit reduction in cursorial perissodactyls [92], and bipedalism in many saltatorial mammals [93]. Many of these specialized mammals may be constrained by their highly derived morphology and thus are adapted to optimize performance for just a single specialized locomotor behavior. That is, most locomotor modes cannot be maximized simultaneously and must trade off with other locomotor modes. In contrast, most carnivorans can perform multiple locomotor behaviors well including running, climbing, digging, and swimming. For example, even the most cursorial carnivoran, the cheetah, can climb trees whereas no cursorial ungulate can. Therefore, the relatively flat landscape in carnivorans signals that functional trade-offs among locomotor performances cannot lead to highly derived specializations, which, in turn, may lead to rugged, multi-peak landscapes in other mammals. Instead, this carnivoran topology highlights that the even slight functional trade-offs across smooth, gradual gradients among appendicular and axial functional traits can facilitate diverse locomotor modes as well as be flexible enough to enable additional locomotor behaviors. Future work “zooming out” of the carnivoran landscape will further elucidate how the relationships

among functional trade-offs, relative degrees of morphological and ecological specializations, and landscape topologies differ among the various clades across Mammalia.

Acknowledgements

We are grateful to the staff and collections at the American Museum of Natural History, California Academy of Sciences, Field Museum of Natural History, Natural History Museum of Los Angeles County, Museum of Vertebrate Zoology, Natural History Museum London, San Diego Natural History Museum, Texas Vertebrate Paleontology Collection, National Museum of Natural History, and Burke Museum of Natural History and Culture. We thank Stephanie Pierce for helpful discussions about adaptive landscapes, Miriam Zelditch and Dave Polly for suggestions on generating theoretical morphological traits from PCAs, and the Santana lab at UW for helpful discussions.

Funding

Funding was supported by the National Science Foundation (grant no. DBI-2128146) to C.J.L., L.J.H., and Z.J.T.; a University of Texas Early Career Provost Fellowship and Stengl-Wyer Endowment Grant (grant no. SWG-22-02) to C.J.L.; and the European Research Council (Tied2Teeth, grant no. 101054659) to L.J.H.

Authors' contributions

C.J.L.: conceptualization, data curation, formal analysis, funding acquisition, investigation, methodology, resources, validation, visualization, writing—original draft, writing—review and

editing; L.J.H.: funding acquisition, investigation, writing— review and editing; Z.J.T.: funding acquisition, investigation, project administration, writing—review and editing.

Figures

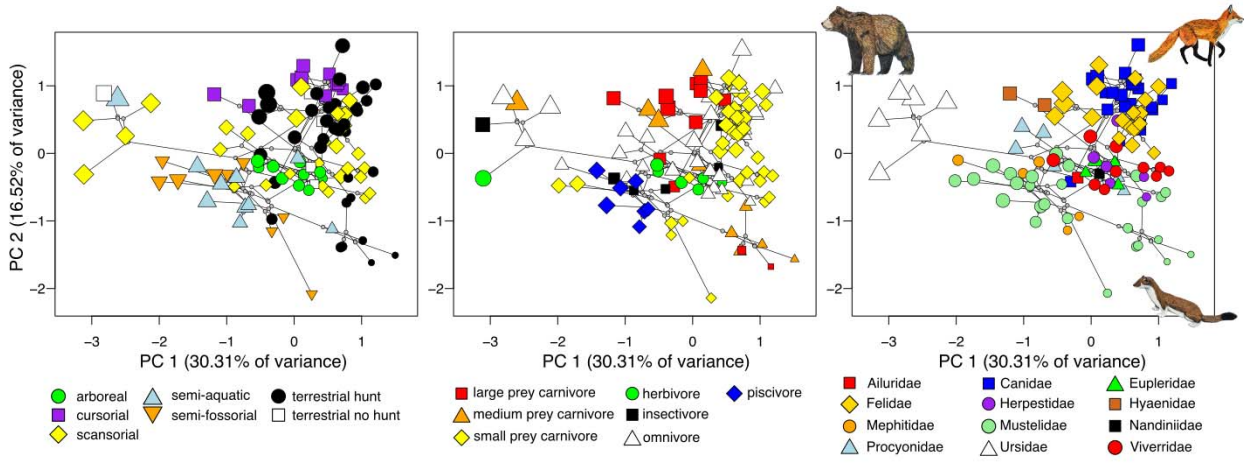

Fig. 1. Phylomorphospace of carnivoran skeletal system defined by principal components (PCs) 1 and 2. PCA was conducted using 136 linear and angular measurements that capture morphological variation across the skull, appendicular, and axial skeletons (Table S1 shows trait loadings). Linear measurements were size-corrected using log shape ratios. Size of points are scaled to estimated body size based on the geometric mean of all measurements.

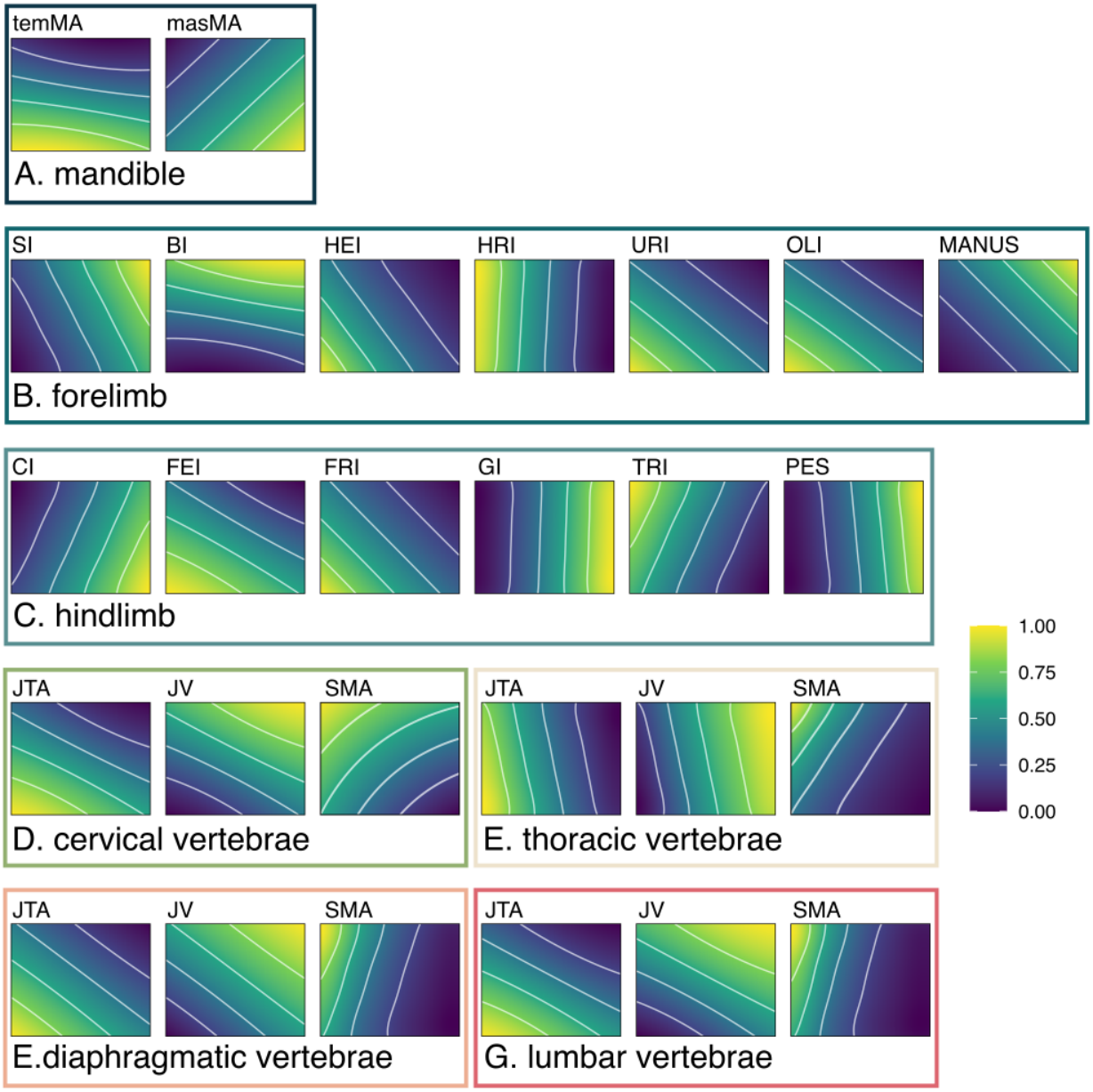

Fig. 2. Performance surfaces for each functional trait. Color represents height on the performance surface. See Table 1 for functional trait definitions.

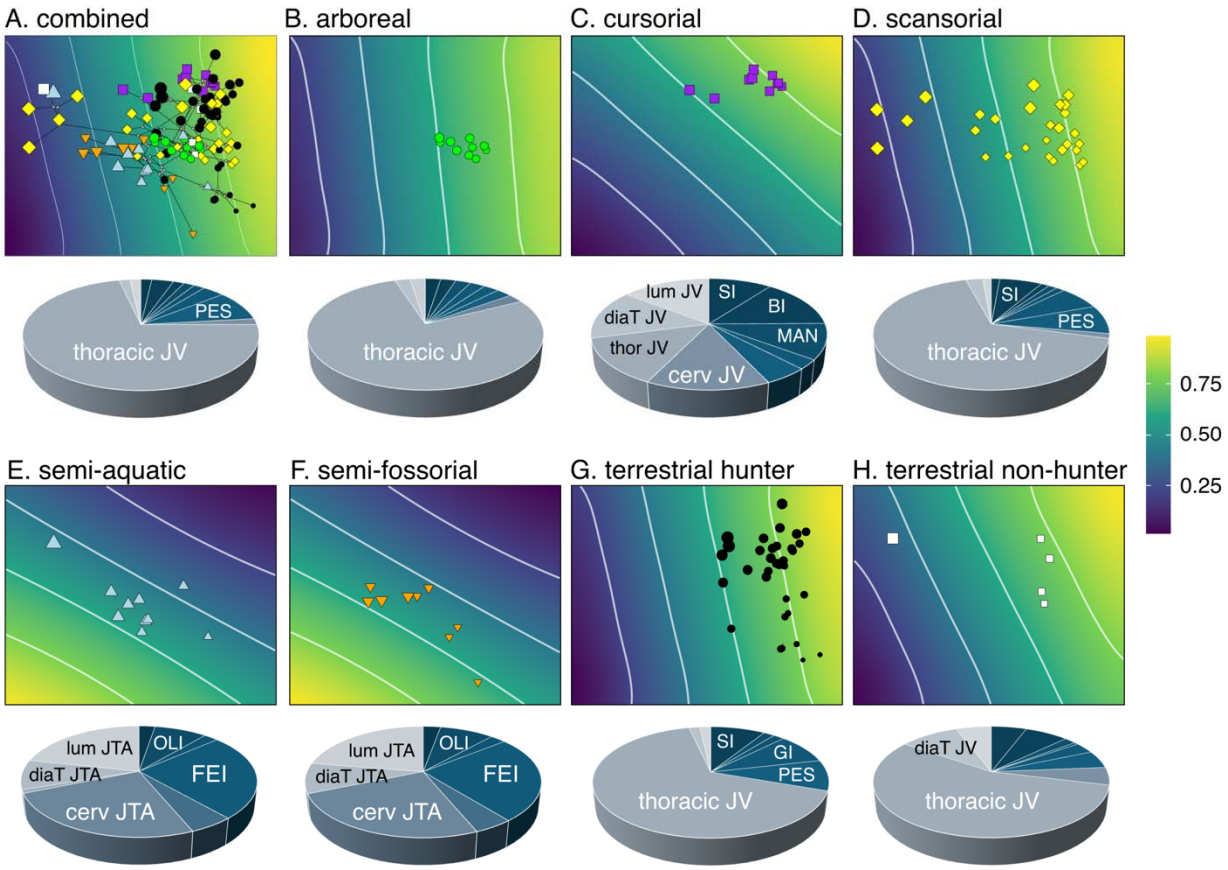

Fig. 3. Adaptive landscapes optimized for all carnivorans and each locomotor group. Landscapes were produced by combining the performance surfaces and optimizing their weightings to maximize the height of the landscape at the group mean. Pie charts show the relative weights of each performance surface on each landscape (Table S2 shows breakdown of weights). Table 2 shows statistical tests comparing adaptive landscapes among locomotor groups. Size of points are scaled to estimated body size based on the geometric mean of all measurements.

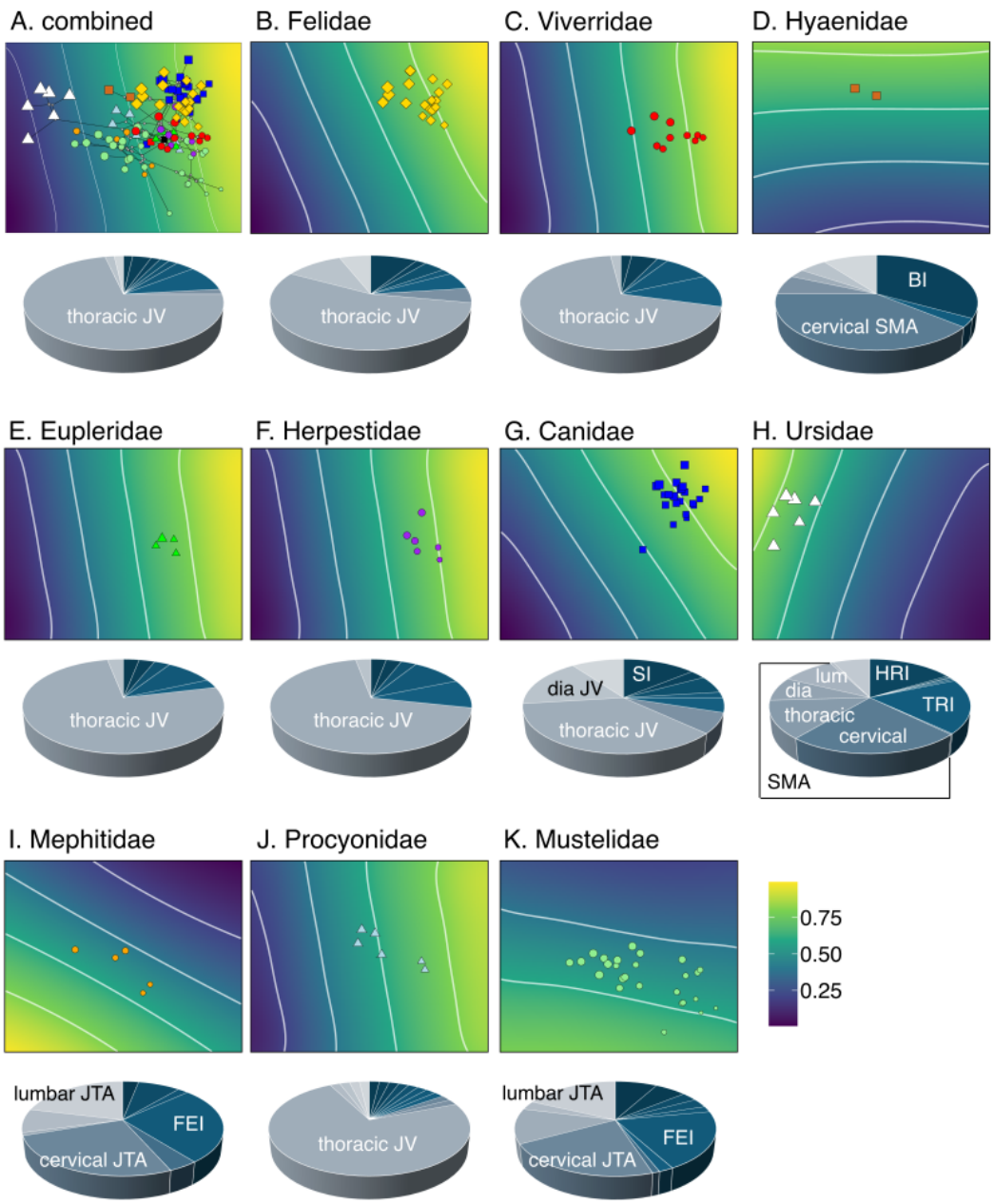

Fig. 4. Adaptive landscapes optimized for all carnivorans and each family. Landscapes were produced by combining the performance surfaces and optimizing their weightings to maximize the height of the landscape at the group mean. Pie charts show the relative weights of each performance surface on each adaptive landscape (Table S5 shows breakdown of weights). Table 3 shows statistical tests comparing adaptive landscapes among families. Size of points are scaled to estimated body size based on the geometric mean of all measurements.

Tables

Table 1. Functional traits capturing the functional diversity of the skull [49], limbs [39,50], and vertebral column [13,51,52].

Functional trait	Definition	Interpretation
Skull		
temporalis mechanical advantage (temMA)	temporalis moment arm / distance from the jaw condyle to the carnassial	Estimates how much force is produced at the bite point from the temporalis muscle.
masseter mechanical advantage (masMA)	masseter moment arm / distance from the jaw condyle to the carnassial	Estimates how much force is produced at the bite point from the masseter muscle.
Forelimb		
Scapula index (SI)	scapula length / scapula height	Describes the expansion of shoulder musculature versus contribution of scapula to limb elongation.
Brachial index (BI)	radius length / humerus length	Estimates relative proportions of proximal and distal elements of the forelimb.
Humeral robustness index (HRI)	mediolateral diameter of humerus / humerus length	Estimates robustness of the humerus and its ability to resist bending and shearing stresses.
Humeral epicondylar index (HEI)	epicondylar breadth of humerus / humerus length	Estimates relative area available for the origins of the forearm flexors, pronators, and supinators.
Olecranon length index (OLI)	olecranon process length / ulna length	Estimates relative mechanical advantage of the triceps brachii and dorsoepitrochlearis muscles used in elbow extension.
Ulnar robustness index (URI)	mediolateral diameter of ulna / ulna length	Estimates robustness of the ulna and its ability to resist bending and shearing stresses, and relative area available for the origin and insertion of forearm and manus flexors, pronators, and supinators.
Manus proportions index (MAN)	metacarpal 3 length / humerus length	Estimates relative proportions of proximal and distal elements of the forelimb, and relative size of the hand.
Hindlimb		

Crural index (CI)	tibia length / femur length	Estimates relative proportions of proximal and distal elements of the hind limb.
Femoral robustness index (FRI)	anteroposterior diameter of femur / femur length	Estimates robustness of the femur and its ability to resist bending and shearing stresses.
Gluteal index (GI)	length of distal extension of the greater trochanter of the femur / femur length	Estimates relative mechanical advantage of the gluteal muscles used in retraction of the femur.
Femoral epicondylar index (FEI)	epicondylar breadth of femur / femur length	Estimates relative area available for the origins of the gastrocnemius and soleus muscles used in extension of the knee and plantar-flexion of the pes.
Tibial robustness index (TRI)	mediolateral diameter of tibia / tibia length	Estimates robustness of the tibia and its ability to resist bending and shearing stresses.
Pes length index (PES)	metatarsal 3 length / femur length	Estimates relative proportions of proximal and distal elements of the hind limb, and relative size of the hind foot.
Vertebrae		
Sagittal second moment of area (sSMA)	π/4 * breadth of posterior centrum * height of the posterior centrum^3	Estimates stiffness in the of the vertebral joint in the sagittal plane.
Lateral second moment of area (lSMA)	π/4 * height of posterior centrum * breadth of the posterior centrum^3	Estimates stiffness in the of the vertebral joint in the lateral plane.
Joint torsional angle (JTA)	360º – absolute value of 270º – angle between postzygapophyses	Estimates the degree of axial torsion of the vertebrae.
Joint verticality (JV)	absolute value of 180º – angle between postzygapophyses	Estimates the relative importance of sagittal bending versus lateral bending of vertebral joints.

Table 2. Pairwise significance tests among locomotor adaptive landscapes. Top triangle: number of landscape models shared in the top 1% between the paired groups. Bottom triangle: P-values for difference between groups. Bolded P-values indicate significance.

	arboreal	cursorial	scansorial	semi-aquatic	semi-fossorial	terrestrial hunter	terrestrial non-hunter
arboreal	-	4	7	0	0	6	6
cursorial	0.400	-	10	0	0	7	34
scansorial	0.700	**0.033**	-	0	0	14	15
semi-aquatic	**0.001**	**0.001**	**0.001**	-	88	0	0
semi-fossorial	**0.001**	**0.001**	**0.001**	0.917	-	0	0
terrestrial hunter	0.600	**0.023**	0.778	**0.001**	**0.001**	-	12
terrestrial nonhunter	0.600	0.114	0.833	**0.001**	**0.001**	0.857	-

Table 3. Pairwise significance tests among familial adaptive landscapes. Top triangle: number of landscape models shared in the top 1% between the paired groups. Bottom triangle: P-values for difference between groups. Bolded P-values indicate significance.

	Nand	Feli	Vive	Hyae	Eupl	Herp	Cani	Ursi	Meph	Ailu	Proc	Must
Nand	-	5	7	0	7	7	5	0	0	7	7	1
Feli	0.714	-	7	0	5	6	35	0	0	5	8	1
Vive	1.000	0.200	-	0	8	10	7	0	0	7	7	1
Hyae	**0.001**	**0.001**	**0.001**	-	0	0	0	0	0	0	0	0
Eupl	1.000	0.143	0.727	**0.001**	-	8	5	0	0	7	7	1
Herp	1.000	0.171	0.909	**0.001**	1.000	-	6	0	0	7	7	1
Cani	0.714	1.000	0.636	**0.001**	0.625	0.600	-	0	0	5	8	1
Ursi	**0.001**	**0.001**	**0.001**	0.059	**0.001**	**0.001**	**0.001**	-	0	0	0	0
Meph	**0.001**	**0.001**	**0.001**	**0.001**	**0.001**	**0.001**	**0.001**	**0.001**	-	0	0	58
Ailu	1.000	0.143	0.636	**0.001**	0.875	0.700	0.053	**0.001**	**0.001**	-	12	8
Proc	1.000	0.229	0.636	**0.001**	0.875	0.700	0.084	**0.001**	**0.001**	0.750	-	4
Must	0.143	**0.029**	0.091	**0.001**	0.125	0.100	**0.011**	**0.001**	0.630	0.500	0.267	-

References

1. Arnold SJ. 1983 Morphology, performance and fitness. *Amer. Zool.* **23**, 347–361. (doi:10.1554/05-647.1)

2. Wainwright PC. 1994 Functional morphology as a tool in ecological research. In *Ecological Morphology Integrative Organismal Biology* (eds PC Wainwright, SM Reilly), Ecological Morphology: Integrative ….

3. Higham TE *et al.* 2021 Linking ecomechanical models and functional traits to understand phenotypic diversity. *Trends in Ecology & Evolution* , 1–14. (doi:10.1016/j.tree.2021.05.009)

4. Law CJ, Duran E, Hung N, Richards E, Santillan I, Mehta RS. 2018 Effects of diet on cranial morphology and biting ability in musteloid mammals. *J. Evol. Biol.* **31**, 1918–1931. (doi:10.1111/jeb.13385)

5. Santana SE, Dumont ER, Dumont E, Davis JL. 2010 Mechanics of bite force production and its relationship to diet in bats. *Funct. Ecol.* **24**, 776–784. (doi:10.1111/j.1365-2435.2010.01703.x)

6. Tseng ZJ, Garcia-Lara S, Flynn JJ, Holmes E, Rowe TB, Dickson BV. 2023 A switch in jaw form–function coupling during the evolution of mammals. *Philos. Trans. R. Soc. B* **378**, 20220091. (doi:10.1098/rstb.2022.0091)

7. Collar DC, Reece JS, Alfaro ME, Wainwright PC. 2014 Imperfect morphological convergence: variable changes in cranial structures underlie transitions to durophagy in moray eels. *Am Nat* **183**, E168–E184. (doi:10.5061/dryad.h9r37)

8. Sustaita D, Pouydebat E, Manzano A, Abdala V, Hertel F, Herrel A. 2013 Getting a grip on tetrapod grasping: form, function, and evolution. *Biol. Rev.* **88**, 380–405. (doi:10.1111/brv.12010)

9. Amson E, Bibi F. 2021 Differing effects of size and lifestyle on bone structure in mammals. *BMC Biol.* **19**, 87. (doi:10.1186/s12915-021-01016-1)

10. Sansalone G, Castiglione S, Raia P, Archer M, Dickson B, Hand S, Piras P, Profico A, Wroe S. 2020 Decoupling Functional and Morphological Convergence, the Study Case of Fossorial Mammalia. *Frontiers Earth Sci* **8**, 112. (doi:10.3389/feart.2020.00112)

11. Dickson BV, Pierce SE. 2019 Functional performance of turtle humerus shape across an ecological adaptive landscape. *Evolution* **73**, 1265–1277. (doi:10.1111/evo.13747)

12. Law CJ, Slater GJ, Mehta RS. 2019 Shared extremes by ectotherms and endotherms: Body elongation in mustelids is associated with small size and reduced limbs. *Evolution* **73**, 735–749. (doi:10.1111/evo.13702)

13. Jones KE, Dickson BV, Angielczyk KD, Pierce SE. 2021 Adaptive landscapes challenge the "lateral-to-sagittal" paradigm for mammalian vertebral evolution. *Curr. Biol.* **31**, 1883-1892.e7. (doi:10.1016/j.cub.2021.02.009)

14. Jones KE, Benitez L, Angielczyk KD, Pierce SE. 2018 Adaptation and constraint in the evolution of the mammalian backbone. *Bmc Evol Biol* **18**, 172. (doi:10.1186/s12862-018-1282-2)

15. Polly PD, Stayton CT, Dumont ER, Pierce SE, Rayfield EJ, Angielczyk KD. 2016 Combining Geometric Morphometrics and Finite Element Analysis with Evolutionary Modeling: Towards a Synthesis. *J Vertebr Paleontol* **36**, e1111225. (doi:10.1080/02724634.2016.1111225)

16. Stayton CT. 2019 Performance in three shell functions predicts the phenotypic distribution of hard□shelled turtles. *Evolution* **73**, 720–734. (doi:10.1111/evo.13709)

17. Arnold SJ, Pfrender ME, Jones AG. 2001 The adaptive landscape as a conceptual bridge between micro- and macroevolution. *Genetica* **112–113**, 9–32. (doi:10.1023/a:1013373907708)

18. Hansen TF. 1997 Stabilizing selection and the comparative analysis of adaptation. *Evolution* **51**, 1341–1351. (doi:10.1111/j.1558-5646.1997.tb01457.x)

19. Butler MA, King AA. 2004 Phylogenetic comparative analysis: a modeling approach for adaptive evolution. *Am Nat* **164**, 683–695. (doi:10.1086/426002)

20. Beaulieu JM, Jhwueng D-C, Boettiger C, O'Meara BC. 2012 Modeling stabilizing selection: Expanding the Ornstein-Uhlenbeck model of adaptive evolution. *Evolution* **66**, 2369–2383. (doi:10.1111/j.1558-5646.2012.01619.x)

21. Uyeda JC, Harmon LJ. 2014 A novel Bayesian method for inferring and interpreting the dynamics of adaptive landscapes from phylogenetic comparative data. *Syst. Biol.* **63**, 902–918. (doi:10.1093/sysbio/syu057)

22. Bastide P, Ané C, Robin S, Mariadassou M. 2018 Inference of Adaptive Shifts for Multivariate Correlated Traits. *Syst. Biol.* **67**, 662–680. (doi:10.1093/sysbio/syy005)

23. Slater GJ. 2022 Topographically distinct adaptive landscapes for teeth, skeletons, and size explain the adaptive radiation of Carnivora (Mammalia). *Evolution* (doi:10.1111/evo.14577)

24. Law CJ. 2022 Different Evolutionary Pathways Lead to Incomplete Convergence of Elongate Body Shapes in Carnivoran Mammals. *Systematic Biol* **71**, 788–796. (doi:10.1093/sysbio/syab091)

25. Friedman ST, Price SA, Hoey AS, Wainwright PC. 2016 Ecomorphological convergence in planktivorous surgeonfishes. *J. Evol. Biol.* **29**, 965–978. (doi:10.1111/jeb.12837)

26. Arbour JH, Curtis AA, Santana SE. 2019 Signatures of echolocation and dietary ecology in the adaptive evolution of skull shape in bats. *Nat Commun* **10**, 2036. (doi:10.1038/s41467-019-09951-y)

27. Price SA, Hopkins SSB. 2015 The macroevolutionary relationship between diet and body mass across mammals. *Biol J Linn Soc* **115**, 173–184. (doi:10.1111/bij.12495)

28. Zelditch ML, Ye J, Mitchell JS, Swiderski DL. 2017 Rare ecomorphological convergence on a complex adaptive landscape: Body size and diet mediate evolution of jaw shape in squirrels (Sciuridae). *Evolution* **71**, 633–649. (doi:10.1111/evo.13168)

29. Dickson BV, Clack JA, Smithson TR, Pierce SE. 2021 Functional adaptive landscapes predict terrestrial capacity at the origin of limbs. *Nature* **589**, 242–245. (doi:10.1038/s41586-020-2974-5)

30. Radinsky LB. 1981 Evolution of skull shape in Carnivores .1. Representative modern Carnivores. *Biol J Linn Soc* **15**, 369–388. (doi:10.1111/j.1095-8312.1981.tb00770.x)

31. Valkenburgh BV. 2007 Deja vu: the evolution of feeding morphologies in the Carnivora. *Amer. Zool.* **47**, 147–163. (doi:10.1093/icb/icm016)

32. Tseng ZJ, Flynn JJ. 2018 Structure-function covariation with nonfeeding ecological variables influences evolution of feeding specialization in Carnivora. *Sci Adv* **4**, eaao5441. (doi:10.1126/sciadv.aao5441)

33. Slater GJ, Friscia AR. 2019 Hierarchy in adaptive radiation: A case study using the Carnivora (Mammalia). *Evolution* **73**, 524–539. (doi:10.1111/evo.13689)

34. Law CJ, Blackwell EA, Curtis AA, Dickinson E, Hartstone□Rose A, Santana SE. 2022 Decoupled evolution of the cranium and mandible in carnivoran mammals. *Evolution* **76**, 2959–2974. (doi:10.1111/evo.14578)

35. Figueirido B, MacLeod N, Krieger J, Renzi MD, Pérez-Claros JA, Palmqvist P. 2011 Constraint and adaptation in the evolution of carnivoran skull shape. *Paleobiology* **37**, 490–518. (doi:10.1666/09062.1)

36. Valkenburgh BV. 1985 Locomotor diversity within past and present guilds of large predatory mammals. *Paleobiology* **11**, 406–428. (doi:10.1017/s0094837300011702)

37. Valkenburgh BV. 1987 Skeletal indicators of locomotor behavior in living and extinct carnivores. *J Vertebr Paleontol* **7**, 162–182. (doi:10.1080/02724634.1987.10011651)

38. Iwaniuk AN, Pellis SM, Whishaw IQ. 1999 The relationship between forelimb morphology and behaviour in North American carnivores (Carnivora). *Can J Zool* **77**, 1064–1074. (doi:10.1139/z99-082)

39. Samuels JX, Meachen JA, Sakai SA. 2013 Postcranial morphology and the locomotor habits of living and extinct carnivorans. *J Morpho* **274**, 121–146. (doi:10.1002/jmor.20077)

40. Martín-Serra A, Figueirido B, Palmqvist P. 2014 A three-dimensional analysis of the morphological evolution and locomotor behaviour of the carnivoran hind limb. *BMC Evol Biol* **14**, 1–13. (doi:10.1186/1471-2148-14-129)

41. Martín-Serra A, Figueirido B, Palmqvist P. 2014 A Three-Dimensional Analysis of Morphological Evolution and Locomotor Performance of the Carnivoran Forelimb. *Plos One* **9**, e85574. (doi:10.1371/journal.pone.0085574)

42. Randau M, Cuff AR, Hutchinson JR, Pierce SE, Goswami A. 2017 Regional differentiation of felid vertebral column evolution: a study of 3D shape trajectories. *Org Divers Evol* **17**, 1–15. (doi:10.1007/s13127-016-0304-4)

43. Figueirido B, Martín-Serra A, Pérez-Ramos A, Velasco D, Pastor FJ, Benson RJ. 2021 Serial disparity in the carnivoran backbone unveils a complex adaptive role in metameric evolution. *Communications Biology* , 1–15. (doi:10.1038/s42003-021-02346-0)

44. Martín-Serra A, Pérez-Ramos A, Pastor FJ, Velasco D, Figueirido B. 2021 Phenotypic integration in the carnivoran backbone and the evolution of functional differentiation in metameric structures. *Evolution Letters* , 1–14. (doi:10.1002/evl3.224)

45. Law CJ. 2021 Ecological drivers of carnivoran body shape evolution. *Am Nat* **198**, 406–420. (doi:10.5061/dryad.pg4f4qrpm)

46. Law CJ. 2021 Evolutionary and morphological patterns underlying carnivoran body shape diversity. *Evolution* **75**, 365–375. (doi:10.1111/evo.14143)

47. Law CJ, Hlusko LJ, Tseng ZJ. 2024 Uncovering the mosaic evolution of the carnivoran skeletal system. *Biol. Lett.* **20**, 20230526. (doi:10.1098/rsbl.2023.0526)

48. Humphreys AM, Barraclough TG. 2014 The evolutionary reality of higher taxa in mammals. *Proc Royal Soc B Biological Sci* **281**, 20132750. (doi:10.1098/rspb.2013.2750)

49. Greaves WS. 2012 The Mammalian Jaw. , 3–25. (doi:10.1017/cbo9781139060851.003)

50. Davis DD. 1964 *The giant panda: a morphological study of evolutionary mechanisms*. Fieldiana (Zoology Memoirs). (doi:10.5962/bhl.title.5133)

51. Jones KE, Gonzalez S, Angielczyk KD, Pierce SE. 2020 Regionalization of the axial skeleton predates functional adaptation in the forerunners of mammals. *Nat Ecol Evol* **4**, 470–478. (doi:10.1038/s41559-020-1094-9)

52. Boszczyk BM, Boszczyk AA, Putz R. 2001 Comparative and functional anatomy of the mammalian lumbar spine. *Anatomical Rec* **264**, 157–168. (doi:10.1002/ar.1156)

53. Muñoz NA. 2020 Locomotion in Rodents and Small Carnivorans: Are they So Different? *Journal of Mammalian Evolution* , 1–12. (doi:10.1007/s10914-020-09515-8)

54. Marshall SK, Spainhower KB, Sinn BT, Diggins TP, Butcher MT. 2021 Hind Limb Bone Proportions Reveal Unexpected Morphofunctional Diversification in Xenarthrans. *J. Mamm. Evol.* **28**, 599–619. (doi:10.1007/s10914-021-09537-w)

55. Hedrick BP, Dickson BV, Dumont ER, Pierce SE. 2020 The evolutionary diversity of locomotor innovation in rodents is not linked to proximal limb morphology. *Scientific Reports* , 1–11. (doi:10.1038/s41598-019-57144-w)

56. Kilbourne BM. 2017 Selective regimes and functional anatomy in the mustelid forelimb: Diversification toward specializations for climbing, digging, and swimming. *Ecol Evol* **66**, 2369–12. (doi:10.1002/ece3.3407)

57. Rickman J, Burtner AE, Linden TJ, Santana SE, Law CJ. 2023 Size And Locomotor Ecology Have Differing Effects on the External and Internal Morphologies of Squirrel (Rodentia: Sciuridae) Limb Bones. *Integr. Org. Biol.* **5**, obad017. (doi:10.1093/iob/obad017)

58. Strang KT, Steudel K. 1990 Explaining the scaling of transport costs: the role of stride frequency and stride length. *J. Zoo□l.* **221**, 343–358. (doi:10.1111/j.1469-7998.1990.tb04006.x)

59. Kram R, Taylor CR. 1990 Energetics of running: a new perspective. *Nature* **346**, 265–267. (doi:10.1038/346265a0)

60. Garland T, Janis CM. 1993 Does metatarsal/femur ratio predict maximal running speed in cursorial mammals? *J. Zoo□l.* **229**, 133–151. (doi:10.1111/j.1469-7998.1993.tb02626.x)

61. Kilbourne BM, Hoffman LC. 2013 Scale Effects between Body Size and Limb Design in Quadrupedal Mammals. *PLoS ONE* **8**, e78392. (doi:10.1371/journal.pone.0078392)

62. Pontzer H. 2007 Effective limb length and the scaling of locomotor cost in terrestrial animals. *J. Exp. Biol.* **210**, 1752–1761. (doi:10.1242/jeb.002246)

63. Pontzer H. 2007 Predicting the energy cost of terrestrial locomotion: a test of the LiMb model in humans and quadrupeds. *J. Exp. Biol.* **210**, 484–494. (doi:10.1242/jeb.02662)

64. Polly PD. 2007 Limbs in mammalian evolution. In *Fins into Limbs Evolution, Development, and Transformation* (ed BK Hall), pp. 245–268. Fins into Limbs Evolution, Development, and Transformation.

65. Hildebrand M. 1985 Digging of Quadrupeds. In *Functional Vertebrate Morphology* (eds M Hildebrand, DM Bramble, KF Liem, DB Wake), pp. 89–109. Cambridge, MA: Harvard University Press. (doi:10.4159/harvard.9780674184404.c6)

66. Nakai D, Fujiwara S. 2023 Fossorial mammals emphasise the forelimb muscle moment arms used for digging: New indices for reconstruction of the digging ability and behaviours in extinct taxa. *J. Anat.* **242**, 846–861. (doi:10.1111/joa.13815)

67. Lessa EP, Stein BR. 1992 Morphological constraints in the digging apparatus of pocket gophers (Mammalia: Geomyidae). *Biol J Linn Soc* **47**, 439–453. (doi:10.1111/j.1095-8312.1992.tb00678.x)

68. Lagaria A, Youlatos D. 2006 ANATOMICAL CORRELATES TO SCRATCH DIGGING IN THE FORELIMB OF EUROPEAN GROUND SQUIRRELS (SPERMOPHILUS CITELLUS). *J Mammal* **87**, 563–570. (doi:10.1644/05-mamm-a-251r1.1)

69. Rose J, Moore A, Russell A, Butcher M. 2014 Functional osteology of the forelimb digging apparatus of badgers. *J. Mammal.* **95**, 543–558. (doi:10.1644/13-mamm-a-174)

70. Fish FE. 2000 Biomechanics and Energetics in Aquatic and Semiaquatic Mammals: Platypus to Whale*. *Physiol Biochem Zool* **73**, 683–698. (doi:10.1086/318108)

71. Samuels JX, Valkenburgh BV. 2008 Skeletal indicators of locomotor adaptations in living and extinct rodents. *J Morpho* **269**, 1387–1411. (doi:10.1002/jmor.10662)

72. Gambaryan PP. 1974 *How Mammals Run: Anatomical Adaptations*. J. Wiley.

73. Schilling N, Hackert R. 2006 Sagittal spine movements of small therian mammals during asymmetrical gaits. *J. Exp. Biol.* **209**, 3925–3939. (doi:10.1242/jeb.02400)

74. Hildebrand M. 1959 Motions of the Running Cheetah and Horse. *J. Mammal.* **40**, 481–495. (doi:10.2307/1376265)

75. Hildebrand M. 1985 Walking and Running. In *Functional Vertebrate Morphology* (eds M Hildebrand, DM Bramble, KF Liem, DB Wake), pp. 38–57. Cambridge, MA: Harvard University Press. (doi:10.4159/harvard.9780674184404.c3)

76. Belyaev RI, Kuznetsov AN, Prilepskaya NE. 2022 From dorsomobility to dorsostability: A study of lumbosacral joint range of motion in artiodactyls. *J. Anat.* **241**, 420–436. (doi:10.1111/joa.13688)

77. Belyaev RI, Kuznetsov AN, Prilepskaya NE. 2021 How the even□toed ungulate vertebral column works: Comparison of intervertebral mobility in 33 genera. *J. Anat.* **239**, 1370–1399. (doi:10.1111/joa.13521)

78. Belyaev RI, Nikolskaia P, Bushuev AV, Panyutina AA, Kozhanova DA, Prilepskaya NE. 2023 Running, jumping, hunting, and scavenging: Functional analysis of vertebral mobility and backbone properties in carnivorans. *J. Anat.* (doi:10.1111/joa.13955)

79. Alexander RMcN, Dimery NJ, Ker RF. 1985 Elastic structures in the back and their rôle in galloping in some mammals. *J. Zoo□l.* **207**, 467–482. (doi:10.1111/j.1469-7998.1985.tb04944.x)

80. McMahon TA. 1985 The role of compliance in mammalian running gaits. *J. Exp. Biol.* **115**, 263–282. (doi:10.1242/jeb.115.1.263)

81. Taylor CR. 1978 Why Change Gaits? Recruitment of Muscles and Muscle Fibers as a Function of Speed and Gait. *Am. Zoo□l.* **18**, 153–161. (doi:10.1093/icb/18.1.153)

82. Koob TJ, Long JH. 2000 The Vertebrate Body Axis: Evolution and Mechanical Function1. *Am. Zoo□l.* **40**, 1–18. (doi:10.1668/0003-1569(2000)040[0001:tvbaea]2.0.co;2)

83. Gál JM. 1993 Mammalian Spinal Biomechanics: I. Static and Dynamic Mechanical Properties of Intact Intervertebral Joints. *J. Exp. Biol.* **174**, 247–280. (doi:10.1242/jeb.174.1.247)

84. Casinos A, Quintana C, Viladiu C. 1993 Allometry and adaptation in the long bones of a digging group of rodents (Ctenomyinae). *Zoo□l. J. Linn. Soc.* **107**, 107–115. (doi:10.1006/zjls.1993.1007)

85. Fish FE. 1994 Association of propulsive swimming mode with behavior in river otters (Lutra canadensis). *J Mammal* **75**, 989–997.

86. Fish FE, Hurley J, Costa DP. 2003 Maneuverability by the sea lion Zalophus californianus: turning performance of an unstable body design. *J. Exp. Biol.* **206**, 667–674. (doi:10.1242/jeb.00144)

87. Oliver JD, Jones KE, Hautier L, Loughry WJ, Pierce SE. 2016 Vertebral bending mechanics and xenarthrous morphology in the nine-banded armadillo (Dasypus novemcinctus). *J. Exp. Biol.* **219**, 2991–3002. (doi:10.1242/jeb.142331)

88. Young JW. 2023 Convergence of arboreal locomotor specialization: morphological and behavioral solutions for movement on narrow and compliant supports. In *Convergent evolution: Animal form and function*, pp. 289–322. Springer International Publishing. (doi:10.1007/978-3-031-11441-0_11)

89. Nations JA, Heaney LR, Demos TC, Achmadi AS, Rowe KC, Esselstyn JA. 2019 A simple skeletal measurement effectively predicts climbing behaviour in a diverse clade of small mammals. *Biol. J. Linn. Soc.* **128**, 323–336. (doi:10.1093/biolinnean/blz085)

90. Wainwright PC, Alfaro ME, Bolnick DI, Hulsey CD. 2005 Many-to-one mapping of form to function: a general principle in organismal design? *Integr Comp Biol* **45**, 256–262. (doi:10.1093/icb/45.2.256)

91. Lin Y-F, Konow N, Dumont ER. 2019 How moles destroy your lawn: the forelimb kinematics of eastern moles in loose and compact substrates. *J. Exp. Biol*. **222**, jeb182436. (doi:10.1242/jeb.182436)

92. Economou G, McGrath M, Wajsberg J, Granatosky MC. 2021 Perissodactyla Locomotion. In *Encyclopedia of Animal Cognition and Behavior* (eds J Vonk, TK Shackelford), pp. 1–8. Switzerland: Springer Nature. (doi:10.1007/978-3-319-47829-6_887-1)

93. McGowan CP, Collins CE. 2018 Why do mammals hop? Understanding the ecology, biomechanics and evolution of bipedal hopping. *J. Exp. Biol.* **221**, jeb161661. (doi:10.1242/jeb.161661)